Spectral Determinations for Discrete Sources with EGRET

E. B. Hughes and P. L. Nolan
W. W. Hansen Laboratories
Stanford University
Stanford, CA 94305

Abstract

The ability of the EGRET telescope to determine the spectral parameters of point sources in 14-day exposures, as planned for the initial survey phase of the GRO mission, is explored by numerical simulation. Results are given for both galactic and extragalactic objects as a function of source strength and for representative levels of diffuse background emission.

I. Introduction

Four of the discrete sources in the second COS-B catalog (Swanenburg *et al.* 1981) have intensities strong enough for spectral measurements to be made in the range 50 MeV to 3 GeV. These are the Crab and Vela pulsars, the source 2CG 195+04 (Geminga), and the quasar 3C273. The pulsed emission from the Crab can be represented by a power law with an index -2.00 ± 0.10 from 50 MeV to 3 GeV (Clear *et al.* 1987), while the pulsed output from Vela is best fitted with an index -1.72 ± 0.07 from 50–300 MeV and a steeper index -2.12 ± 0.07 from 300–3,000 MeV (Grenier, Hermsen, and Clear 1988). The source 2CG 195+04 exhibits a spectral index of -1.8 in the range 100 MeV to 3.2 GeV (Masnou *et al.* 1981), while 3C273 displays a spectral shape that can be characterized by a power law index of $-2.5^{+0.6}_{-0.5}$ in the range 50 MeV to 800 MeV (Bignami *et al.* 1981). The remaining 21 sources identified by COS-B are too weak, relative to the COS-B sensitivity, to permit spectral measurements, but all are broadly consistent with an index of -2.0 when the flux ratio of γ rays above 100 MeV and 300 MeV respectively is examined. In general, the shape of the observed spectrum of high-energy γ rays is expected to be a good indicator of the physical mechanism responsible for their production.

Just as the EGRET telescope, due to its larger effective area, improved directional sensitivity and better energy resolution, is expected to be able to detect discrete γ ray sources with a threshold sensitivity approximately a factor of 20 below that of COS-B, so should EGRET also, for the same reasons, be able to provide spectral determinations for sources weaker than the four already characterized. In this note, for the source strengths accessible to EGRET, we examine the precision of the spectral determinations that should be forthcoming.

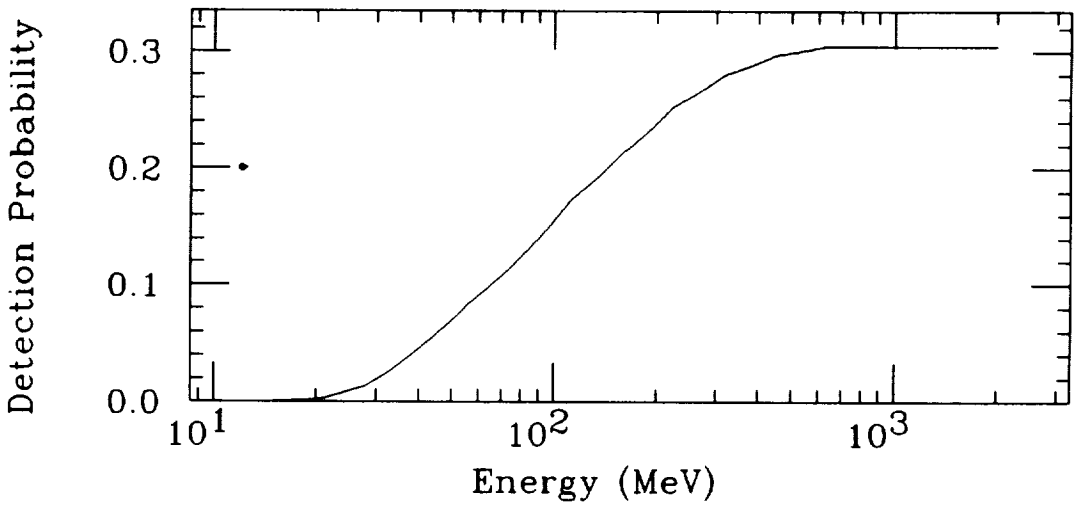

Figure 1: Approximate EGRET detection efficiency used in the simulations. The maximum efficiency of 0.3 corresponds to an effective area of 2000 cm^2.

II. Method

Our method of analysis is to simulate an EGRET observation, typically for a 14-day period, under the assumption that both the point source and the local diffuse background are characterized by a power law emission spectrum $I(E) = AE^{-\alpha}$. This observation is then analyzed to determine the source parameters A and α. By repetition of the EGRET simulation and parameter determination, usually for 100 trials, the measured uncertainties on the parameters A and α are established.

The EGRET efficiency for γ-ray detection is assumed to vary with energy as shown in Figure 1, and the lineshape for γ-ray energy measurement to be as shown in Figure 2. The EGRET angular resolution for γ rays, projected onto one transverse dimension, is assumed to follow the power law $\sigma_{rms}(E) = k(E/1\,\mathrm{MeV})^{-0.6}$ with $k = 56°$. This is accommodated in the spectral simulations by defining an acceptance cone, of half angle $\theta(E)$, relative to the source direction. The width of this cone is taken as proportional to $\sigma_{rms}(E)$ with a proportionality constant C. The fraction of source counts f accepted at any energy by the cone is then $f = 1 - e^{-C^2/2}$, which for $C = 1.5$ is 0.68. The EGRET characteristics just defined are not those that will eventually emerge from a detailed analysis of the EGRET calibration data. They are simply approximations made for the purpose of the present calculations. For example, they do not reflect the probable exclusion of edge events with degraded energy resolution or a possible reduction in detection efficiency at the highest energies due to self-veto from backscattered soft photons.

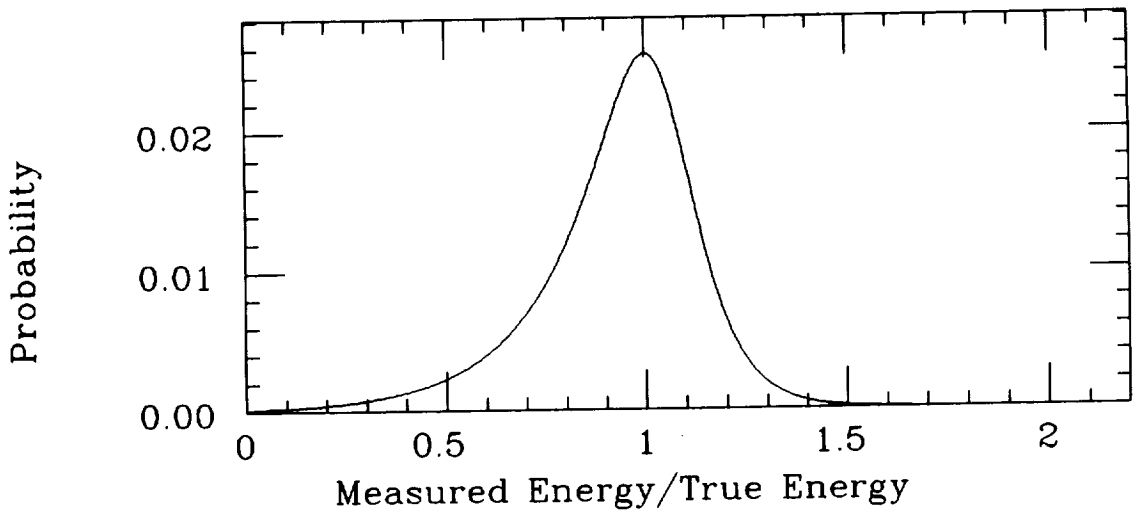

Figure 2: Approximate EGRET energy response function used in the simulation.

Consider the simulation of a point source equal in intensity to the pulsed emission from the Crab; viz. $I(E) = 4.8 \times 10^{-4} E^{-2.10}$ γ rays $\mathrm{cm}^{-2}\mathrm{s}^{-1}\mathrm{MeV}^{-1}$. The observing time is 14 days, the duty factor (due to earth occultation and SAA transits) is 50%, the maximum EGRET effective area is 2000 cm^2 and the acceptance cone efficiency is 68%. The mean number of incident γ rays during this observation, N, is first obtained by analytical integration. Thereafter, for each simulation, the actual number of incident γ rays is randomized with a variance of N. The simulation is carried out by randomly selecting γ rays from the assumed spectrum and, for each such γ ray, consulting Figure 1 to decide, in a random way, if the γ ray is detected. For detected γ rays the measured energy is assigned by random selection from the resolution function specified in Figure 2 and the event is assigned to an appropriate energy bin.

In addition to the source, an overlapping diffuse background is also in general detected. Simulation of this background flux proceeds as for the source itself with the assumption that its strength, at all energies, is constant over the relevant acceptance cone of the instrument. The number of background γ rays at any energy, unlike the source, is proportional to the solid angle of the acceptance cone. This means that if the source and background have similar spectral shapes, the ratio of source to background counts increases rapidly with increasing γ ray energy.

Table I shows the average number of source and background counts obtained for the simulation of a source with Crab-like intensity in the presence of a background typical of the Crab environment. The counts are distributed in 20 bins of logarithmically increasing

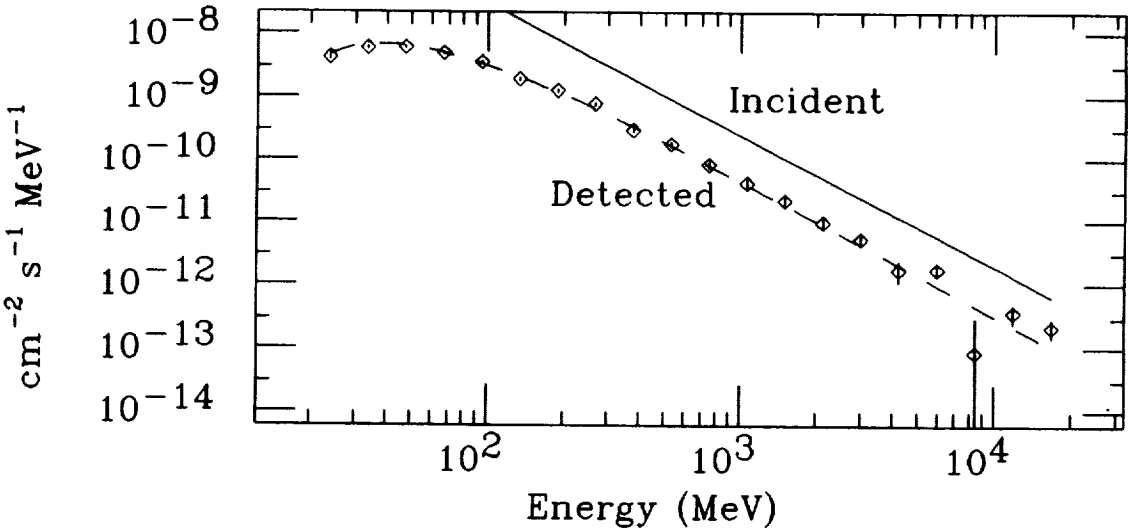

Figure 3: A typical simulation of the measured spectrum of a source with Crab-like intensity and background.

width over the nominal EGRET range of 20–20,000 MeV. The simulation actually extends to energies above and below this range, to reproduce properly the population of the extreme bins due to the EGRET energy lineshape.

In the analysis of a simulated EGRET observation, the first step is to subtract from the observed spectrum (source plus background) an estimate of the measured background. The latter is obtained by simulating the background spectrum many times, usually for 1,000 trials, and taking the mean. The resultant statistical errors in the mean spectrum are thus very small. This is justified because, in principle, for any EGRET observation the overlapping background can be deduced from a statistical analysis or modelling of the relatively large background field surrounding the source that will also be observed. The result of a simulation for a source with Crab-like intensity in the presence of a background typical of the galactic anticenter region is shown in Figure 3.

The source parameters are determined by minimizing the function

$$\chi^2 = \sum_j w_j (n_j - b_j - C_j(A, \alpha))^2, \tag{1}$$

where the summation extends over the energy bins defined by the observation, n_j is the number of photons observed in energy bin j, b_j is the expected number of background counts, $C_j(A, \alpha)$ is the expected number of counts due to the trial source spectrum, and $w_j = n_j^{-1}$ is a weighting factor. The use of this weighting factor actually introduces a

Bin	Energy (MeV)	Source counts	Bkgd. counts
1	20–28	143.5	584.1
2	–40	293.6	892.4
3	–56	404.8	883.8
4	–80	437.0	666.9
5	–112	422.2	430.9
6	–159	370.4	257.5
7	–224	305.7	142.1
8	–317	237.7	74.6
9	–448	174.3	35.7
10	–632	123.7	17.1
11	–893	86.7	8.2
12	–1262	58.3	4.0
13	–1783	39.8	1.7
14	–2518	27.1	0.9
15	–3557	18.5	0.4
16	–5024	12.9	0.2
17	–7096	8.5	0.1
18	–10024	5.8	0.0
19	–14159	4.2	0.0
20	–20000	2.9	0.0
	20–20000	3177.3	4000.6

Table I: Average source and background counts for a Crab-like observation.

small bias in α when bin populations $n_j < 10$ are involved. The effect is to produce a best-fit model spectrum slightly steeper than the known input spectrum. Our simulations show that this bias in α is comparable in size to the statistical error, or smaller. It may be reduced by repeating the analysis with $w_j = (C_j + b_j)^{-1}$, with C_j taken from the first iteration. This was not done for the simulations reported here because the problem has very little effect on the size of the uncertainties in α, which are the main objective of this study.

In principle, $C_j(A, \alpha)$ is given by

$$C_j(A, \alpha) = \int_0^\infty G\varepsilon(E) R_j(E) A E^{-\alpha} dE, \tag{2}$$

where $R_j(E)$ is the probability of assigning a detected γ ray of energy E to the jth bin, $\varepsilon(E)$ is the detector efficiency shown in Figure 1, and G is the EGRET geometric area of $\sim 6500\text{cm}^2$. In particular, for an arbitrary energy resolution function, it is simpler to

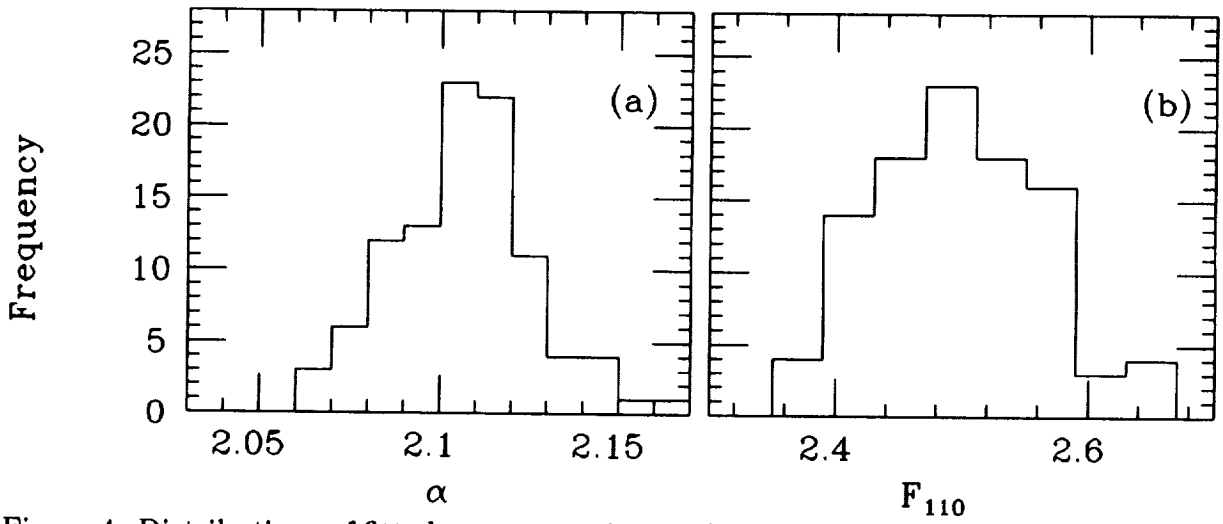

Figure 4: Distributions of fitted parameters in simulations of the Crab: (a) Spectral index α (mean 2.107, standard deviation 0.020). (b) Flux at 110 MeV ($= A \times 110^{-\alpha}$) in units of $10^{-8}\mathrm{cm}^{-2}\mathrm{s}^{-1}\mathrm{MeV}^{-1}$.

obtain C_j by numerical integration, whereby

$$C_j(A,\alpha) = \sum G R_{ij} \varepsilon_i A E_i^{-\alpha} \Delta E_i. \tag{3}$$

R_{ij} is an EGRET response matrix that specifies the probability that a detected γ ray of energy E_i will be found in the bin E_j. R_{ij} is obtained in a separate calculation in which the energy response function is integrated over a set of 270 bins for true energy and typically 20 bins or fewer for observed energy. The true energy bins are chosen to be narrower than the instrument energy response function, so that R_{ij} is independent of the incident spectrum.

Repetition of the above procedure provides a distribution function for the parameters A and α from which both the mean and uncertainty of their determinations can be obtained. These distributions, for the simulation of the source with Crab-like strength and Crab-like background, are reproduced in Figure 4. The correlation between the parameters is reduced by normalizing the spectrum at the intermediate energy of 110 MeV.

III. Results

A summary of the estimated precision with which the spectral index α can be determined in a 14-day EGRET observation is shown in Figure 5 for representative galactic

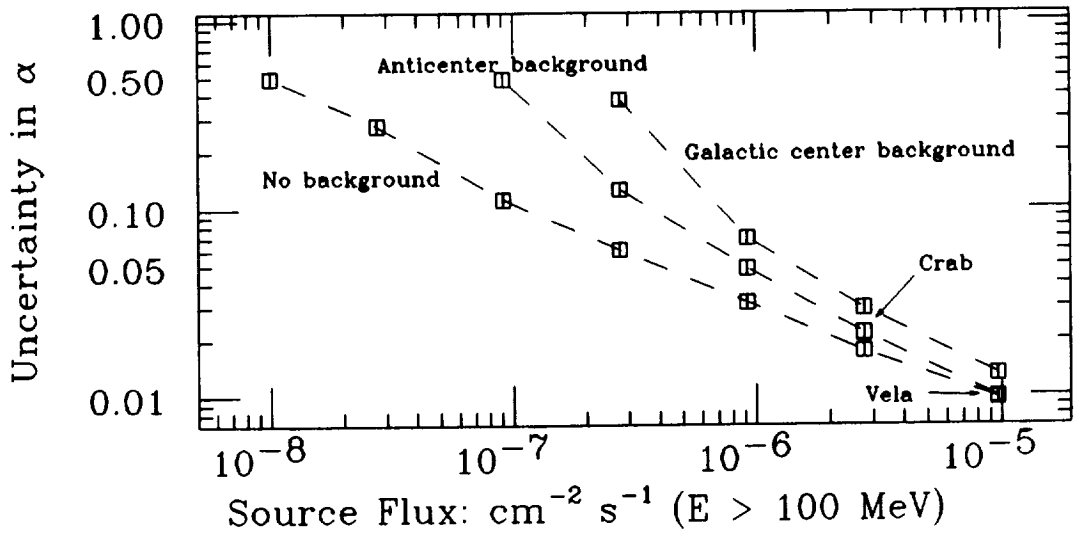

Figure 5: Statistical uncertainty in spectral index for galactic sources as a function of source strength for different diffuse backgrounds.

point sources. The simulated observations are generated for sources and backgrounds with a spectral index of 2.1 and results are given both as a function of the source intensity and the level of diffuse background. The influence of the latter is exhibited through the use of background intensities characteristic of the galactic center and anticenter regions, and also, for reference, in the absence of a background. For example, Figure 5 shows that the spectral index for a source of Vela-like intensity (10^{-5}cm^{-2}s^{-1} ($E > 100$ MeV)) observed against a galactic anticenter background should be measureable, from a statistical standpoint, with an uncertainty close to about 0.01. This result corresponds to the detection of 11,112 source and 3,997 background counts in the range 20–20,000 MeV. For comparison, in a total elapsed observing time of 300 days COS-B was able to detect 2,412 source and 828 background counts in the range 50–5,000 MeV and thereby determine the Vela spectral index to an uncertainty of 0.07. Similarly, a single 14-day EGRET observation of a source with Crab-like intensity (2.8×10^{-6}cm^{-2}s^{-1}(E > 100 MeV)) with 2,177 source counts and 3,997 background counts should yield α with an uncertainty of 0.02, whereas it required 175 days of exposure, resulting in the detection of 800 source and 900 background counts, for COS-B to determine α to within 0.1. These results suggest that, with EGRET, it should be possible to search for variations in the Crab and Vela spectra, and also weaker sources, as a function of binary phase and epoch with good sensitivity.

For sources of intensity 10^{-6}cm^{-2}s^{-1} (E > 100 MeV) the spectral index is measureable by EGRET to a precision of 0.05–0.07, depending upon the background level. Such

sources are at the COS-B threshold of detectability and are too weak for COS-B to provide index measurements. For sources of strength $10^{-7}cm^{-2}s^{-1}$ (E > 100 MeV), close to the EGRET threshold of detectability, the index for those in the anticenter region is measureable to within 0.5 in 14 days. At this source strength, the measurement error becomes very sensitive to the background level and, as indicated in Figure 5, the precision of the index determination is significantly reduced as the background approaches that typical of the galactic center. The mean number of source counts that will be detected for this source strength is 397, whereas the background counts will range from 3,997 in the anticenter region to 21,320 in the galactic center region. The distribution of the detected source counts with energy may be obtained by scaling from Table I, but are reproduced, for convenience, in Table II for sources of strength 10^{-6} and $10^{-7}cm^{-2}s^{-1}$ ($E > 100$ MeV).

Bin	Energy (MeV)	Crab counts	10^{-6} counts	10^{-7} counts
1	20–28	143.5	51.2	5.1
2	–40	293.6	104.9	10.5
3	–56	404.8	144.6	14.5
4	–80	437.0	156.1	15.6
5	–112	422.2	150.8	15.1
6	–159	370.4	132.2	13.2
7	–224	305.7	109.2	10.9
8	–317	237.7	84.9	8.5
9	–448	174.3	62.2	6.2
10	–632	123.7	44.2	4.4
11	–893	86.7	31.0	3.1
12	–1262	58.3	20.8	2.1
13	–1783	39.8	14.2	1.4
14	–2518	27.1	9.7	1.0
15	–3557	18.5	6.6	0.7
16	–5024	12.9	4.6	0.5
17	–7096	8.5	3.0	0.3
18	–10024	5.8	2.1	0.2
19	–14159	4.2	1.5	0.2
20	–20000	2.9	1.0	0.1
	20–20000	3177.3	1134.8	113.5

Table II: Average source counts for Crab-like and weaker sources of 10^{-6} and $10^{-7}cm^{-2}s^{-1}$ ($E > 100$ MeV). The associated background counts are identical to those given in Table I for each source.

If the duration of an EGRET observation is extended from 2 weeks to 10 weeks, then the limitations imposed by the diffuse background, especially in the galactic center region,

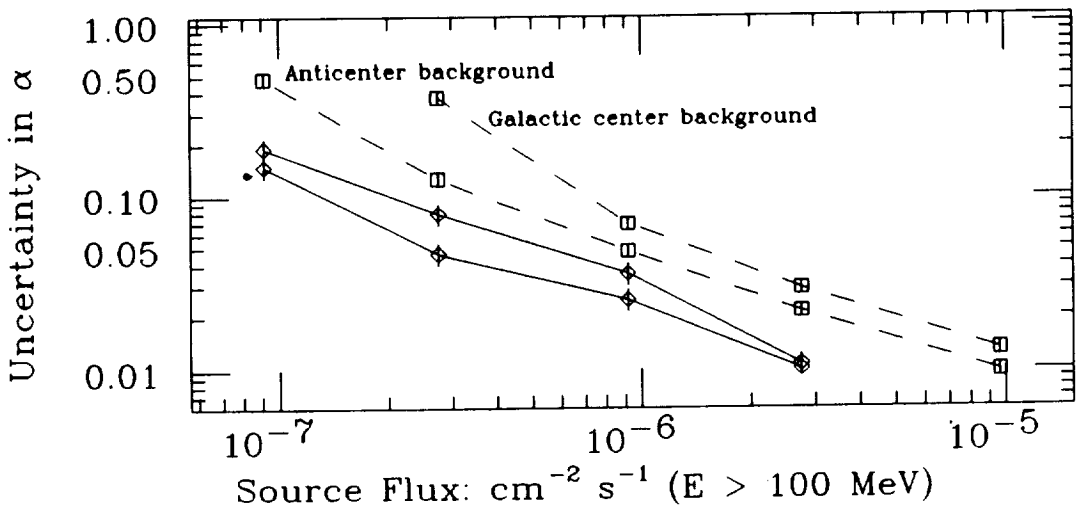

Figure 6: Uncertainty in measurement of spectral index for galactic sources as a function of observing time. Dashed lines: 2-week observations. Solid lines: 10-week observations.

are much reduced. A comparison of the results obtained for these two observing times at the two representative levels of diffuse background is shown in Figure 6. For sources of intensity close to 10^{-7}cm^{-2}s^{-1} (E > 100 MeV), the spectral index is measureable with an uncertainty of about 0.2.

The spectrum of the extragalactic source 3C273 was found by COS-B to be consistent with a power law index of $2.5^{+0.6}_{-0.5}$. The total observing time was 71 days. The EGRET capability, in 14-day observing periods, for representative extragalactic objects with a spectral index of 2.5 is indicated in Figure 7. In a single observation, for a source of 3C273-like intensity (7×10^{-7} cm^{-2}s^{-1} ($E > 100$MeV)), the spectral index is measureable to a precision of close to 0.05. The variation of this measurement error with source intensity and background level is given in Figure 7. This figure indicates that EGRET should be able to obtain useful spectrum measurements for extragalactic sources one tenth as strong as 3C273.

Another measure of the EGRET capability is the degree to which departures from the simple power law shape can be detected. Evidence for such a departure has been provided by the COS-B observations (Grenier, Hermsen and Clear 1988) which suggest, for the Vela pulsar, a spectral break at about 300 MeV. The preferred spectral index in the range 50–300 MeV is 1.72 ± 0.07, whereas in the range 300–5,000 MeV it is 2.12 ± 0.07. An indication of the detectability of such spectral breaks by EGRET is provided by the results summarized in Figure 8(a). These results are obtained by simulating a source of

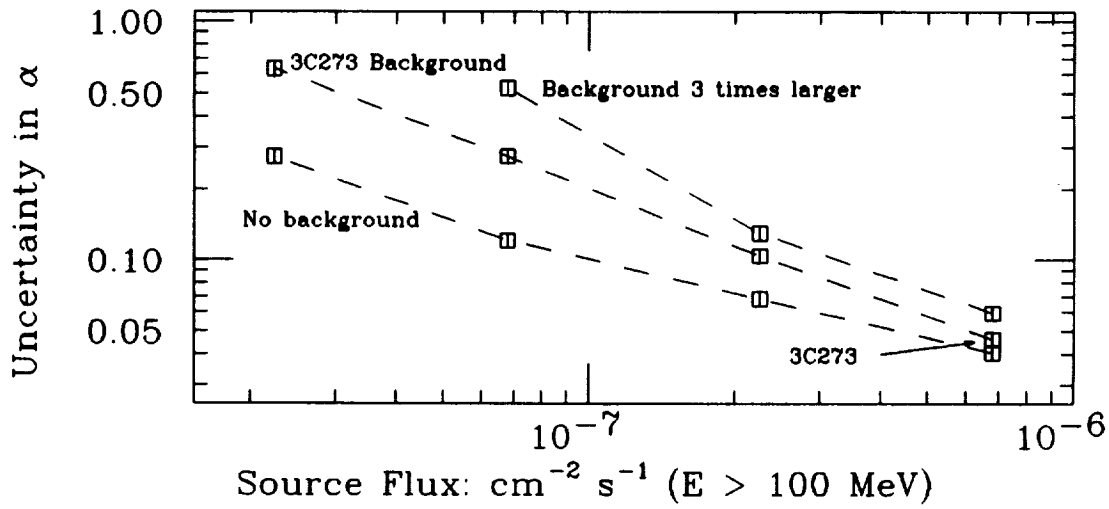

Figure 7: Statistical uncertainty in spectral index for representative extragalactic sources as a function of source strength for different diffuse backgrounds.

Crab-like intensity with a spectral break at a specified energy in the range 100–1,000 MeV. The goodness of fit to a single power law index (averaged over 30 trials) is displayed as a function of the spectral index encountered above each of the assumed break energies. Also indicated, by the dashed horizontal lines, is the confidence level with which a spectral break can be established. For example, a spectral break at 300 MeV for a source of Crab-like strength should be detectable with 95% confidence if it exceeds 0.1 in magnitude. Similar results for a source with the characteristics of 3C273 are given in Figure 8(b). The variations of the sensitivity to a spectral break with break energy revealed in Figure 8 reflect the hardness of the spectrum of each source. EGRET is least sensitive to a break at 100 MeV in the hard Crab spectrum, but it is least sensitive at 1000 MeV in the softer 3C273 spectrum.

The results in Figures 8 are summarized in a more compact fashion in Figure 9. Here the index change that can be detected with 95% confidence is shown for both the Crab and 3C273 sources as a function of the energy at which the index change occurs. These results refer to standard 14-day EGRET observations. If the observing period is longer, then improved sensitivity is achieved. Figure 10 shows the sensitivity expected for 3C273 and for galactic sources of strength 10% of the Crab if the observing period is increased to 10 weeks.

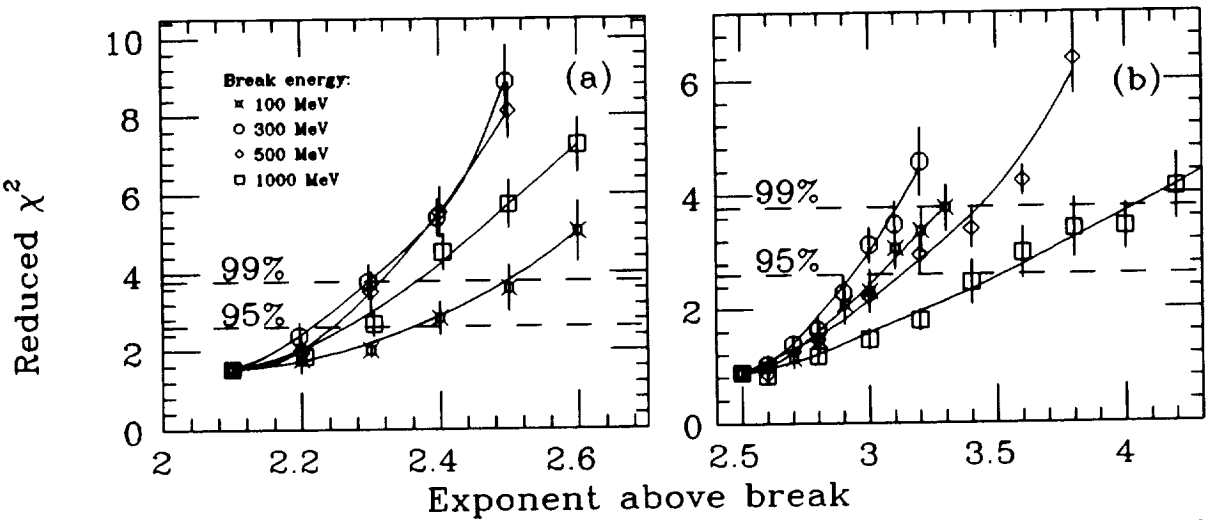

Figure 8: Goodness of fit for broken power law spectra when the fitting model is a single power law. The various curves correspond to different break energies. These simulations were done with 5 energy bins, so χ^2 has 3 degrees of freedom. (a) Crab. (b) 3C273.

IV. Summary

A quantitative exploration has been made of the capability of the EGRET telescope to measure the spectral shapes of high-energy γ-ray sources in the range 20–20,000 MeV. Using a simple power law as a reference spectrum, it is shown that for galactic objects equal in strength to 10% of the pulsed Crab emission the power law index should be measureable to better than 0.2 in the anticenter region and to a precision of about 0.4 in the galactic center region in a typical observing time of 14 days. If this observing time is extended to 10 weeks then the level of precision should be in the range 0.04 to 0.08 depending upon the local background intensity. As the source strength S increases, the precision should improve, from a statistical standpoint, approximately as $S^{-1/2}$. For extragalactic objects equal in intensity to 10% of 3C273 and in background fields typical of the 3C273 environment, the spectral index should be measurable to about 0.3 in 14-day exposures. The level of precision for such objects is also examined as a function of source and background intensity. Finally, in anticipation of emission spectra more complex than the simple power law, the detectability of index changes at specific energies in power law spectra is quantified.

All of the uncertainties reported above are purely statistical. In practice, it will be necessary to be alert to systematic errors that could affect the determination of spectral parameters. These include changes over time in the detector efficiency with energy.

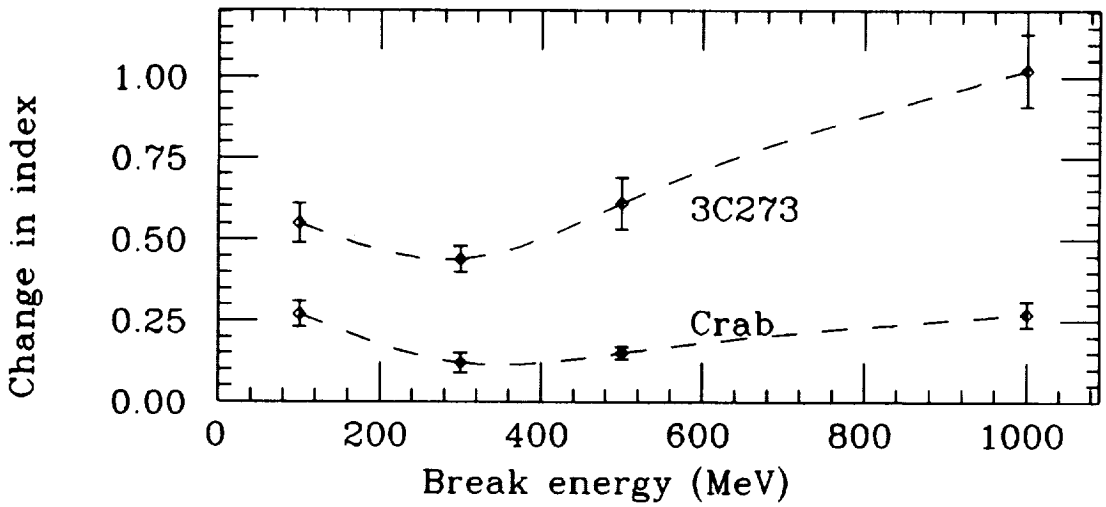

Figure 9: Minimum spectrum break detectable in 2 weeks with 95% confidence for Crab-like and 3C273-like spectra below the break.

To a lesser degree, the statistical fluctuations in the calibration of the efficiency and energy response function will also affect the results in a systematic way. The results also depend on the assumed parametrization of the EGRET efficiency, energy resolution, and angular resolution. The latter, in particular, determines the number of background counts detected and becomes increasingly important as the source strength decreases.

We are pleased to acknowledge the many useful contributions to this work by Stanford student Mark Fardal and by San Francisco State University students Craig Searcy and Martin Krockenberger. This work was supported by NASA contract NAS5-27557.

References

Bignami, G. F., Bennett, K., Buccheri, R., Caraveo, P. A., Hermsen, W., Kanbach, G., Lichti, G. G., Masnou, J. L., Mayer-Hasselwander, H. A., Paul, J. A., Sacco, B., Scarsi, L., Swanenburg, B. N., and Wills, R. D. 1981, *Astron. Astrophys.*, **93**, 71.

Clear, J., Bennett, K., Buccheri, R., Grenier, I. A., Hermsen, W., Mayer-Hasselwander, H. A., and Sacco, B. 1987, *Astron. Astrophys.*, **174**, 85.

Grenier, I. A., Hermsen, W., and Clear, J. 1988, *Astron. Astrophys.*, **204**, 117.

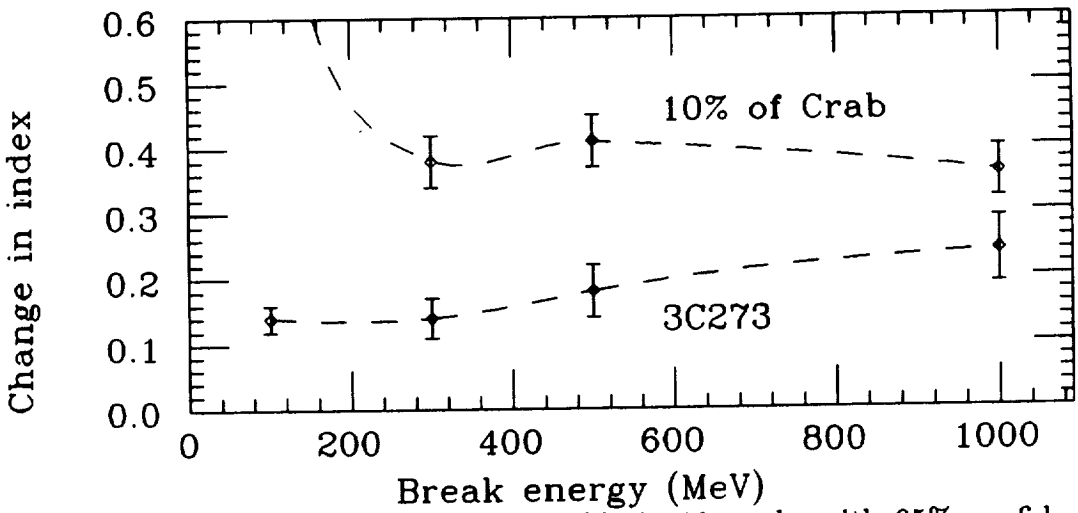

Figure 10: Minimum spectrum break detectable in 10 weeks with 95% confidence for sources with 3C273-like and 10% Crab-like spectra below the break. A break at 100 MeV or below is not detectable in the Crab-like source.

Masnou, J. L., Bennett, K., Bignami, G. F., Bloemen, J. B. G. M., Buccheri, R., Caraveo, P. A., Hermsen, W., Kanbach, G., Mayer-Hasselwander, H., Paul, J. A., and Wills, R. D. 1981, *17th International Cosmic Ray Conference,* paper XG4.3-12, **1**, 177.

Swanenburg, B. N., Bennett, K., Bignami, G. F., Buccheri, R., Caraveo, P., Hermsen, W., Kanbach, G., Lichti, G. G., Masnou, J. L., Mayer-Hasselwander, H. A., Paul, J. A., Sacco, B., Scarsi, L., and Wills, R. D. 1981, *Ap. J.,* **243**, L69.

Bursts and Solar Flares